



**HAL**  
open science

## Investigation of the potential of the ICP-MS/MS for total and speciation analysis in petroleum fractions

Fabien Chainet, Alain Desprez, Sylvain Carbonneaux, Linda Ayouni,  
Marie-Laure Milliand, Charles-Philippe Lienemann

► **To cite this version:**

Fabien Chainet, Alain Desprez, Sylvain Carbonneaux, Linda Ayouni, Marie-Laure Milliand, et al.. Investigation of the potential of the ICP-MS/MS for total and speciation analysis in petroleum fractions. Fuel Processing Technology, 2019, 188, pp.60-69. 10.1016/j.fuproc.2019.01.013 . hal-02091325

**HAL Id: hal-02091325**

**<https://ifp.hal.science/hal-02091325>**

Submitted on 5 Apr 2019

**HAL** is a multi-disciplinary open access archive for the deposit and dissemination of scientific research documents, whether they are published or not. The documents may come from teaching and research institutions in France or abroad, or from public or private research centers.

L'archive ouverte pluridisciplinaire **HAL**, est destinée au dépôt et à la diffusion de documents scientifiques de niveau recherche, publiés ou non, émanant des établissements d'enseignement et de recherche français ou étrangers, des laboratoires publics ou privés.

# Investigation of the potential of the ICP-MS/MS for total and speciation analysis in petroleum fractions

Fabien Chainet<sup>1</sup>, Alain Desprez<sup>2</sup>, Sylvain Carbonneaux<sup>1</sup>, Linda Ayouni<sup>3</sup>, Marie-Laure Milliand<sup>3</sup>, Charles-Philippe Lienemann<sup>1\*</sup>

1: IFP Energies nouvelles, Rond-point de l'échangeur de Solaize, BP3, 69360 Solaize, France

2: Agilent Technologies France, Parc Technopolis – ZA Courtaboeuf, 3 avenue du Canada, F-91978 Les Ulis

3: Université de Lyon, Institut des Sciences Analytiques, UMR 5280 (CNRS, Université Lyon 1, ENS Lyon) - 5, rue de la Doua, F-69100 Villeurbanne, France

## Abstract

The capability of inductively coupled plasma tandem mass spectrometry (ICP-MS/MS) to achieve total concentration and speciation using direct injection of petroleum products after solvent dilution for severely interfered isotopes was demonstrated here with different applications cases. For the direct determination of heavy elements ( $Z > 70$ ) in organic matrices, the ICP-MS/MS was less sensitive than the ICP-HRMS. For light elements ( $Z < 40$ ), the sensitivity was similar or better using ICP-MS/MS and for interfered elements (Si, S, Ca, Fe), the use of the two quadrupoles combined to the octopole reaction/collision cell (ORC) with He, O<sub>2</sub> or H<sub>2</sub> gave similar or better detection limits (LOD) than the ICP-HRMS in medium resolution. Comparable or better sensitivity were obtained replacing the 1.5 mm by the 1 mm injector diameter and especially for lighter elements ( $Z < 30$ ) using the ICP-MS/MS. LOD in xylene were ranging from 0.004 μg/kg (V) to 0.9 μg/kg (Al) and appeared in the lowest values published in the literature using ICP-MS/MS in hydrocarbons. To demonstrate the performance of the ICP-MS/MS using direct injection of petroleum products after dilution in hydrocarbon solvent, three application cases were presented.

Sulfur at very low levels in reformates was successfully monitored in oxygen mode using the oxide ion ( $^{32}\text{S} \rightarrow ^{48}\text{SO}$ ). The background equivalent concentration (BEC) origin was attributed to solvent contamination by sulfur and was confirmed by ultra-violet fluorescence (UVF) method. Using H<sub>2</sub> for Ni ( $^{58}\text{Ni} \rightarrow ^{58}\text{Ni}$ ) and O<sub>2</sub> for V ( $^{51}\text{V} \rightarrow ^{67}\text{VO}$ ) as reactant gas, the direct injection ICP-

31 MS/MS method easily confirmed Ni and V concentrations measured using wavelength dispersive  
32 X-rays fluorescence (WDXRF) and allowed the determination of 14 elements in the asphaltene  
33 fraction, with concentrations ranging from 0.3 mg/kg (Al and Pb) to 37.4 mg/kg for Fe.  
34 For speciation of Ni, V and S, gel permeation chromatography (GPC) hyphenated to ICP-MS/MS  
35 is particularly powerful using O<sub>2</sub> (2.5 mL/min) both for vacuum residue and hydrotreated (HDT)  
36 vacuum residue. Contrary to GPC-ICP-HRMS where two injections of sample were required  
37 (medium resolution for S and V and low resolution for Ni), GPC-ICP-MS/MS easily allowed the  
38 acquisition of the 3 elements in one mode during the same run and considerably reduce the  
39 analysis cost and time. Both for total and speciation analysis, the direct injection after solvent  
40 dilution ICP-MS/MS method is a significant advantage and appealing in high-volume petroleum  
41 laboratories.

42  
43 **Keywords :** trace analysis; detection limits; speciation; petroleum products; polyatomic  
44 interferences; ICP-MS/MS; ICP-HRMS; GPC; vacuum residue

45  
46

47	<b>1</b>	<b>INTRODUCTION</b> .....	<b>4</b>
48	<b>2</b>	<b>MATERIALS AND METHODS</b> .....	<b>7</b>
49	2.1	SOLUTIONS AND SAMPLES .....	7
50	2.2	INSTRUMENTATION .....	8
51	2.2.1	ICP-MS and GPC-ICP-MS .....	8
52	2.2.2	UVF and XRF apparatus .....	11
53	<b>3</b>	<b>RESULTS AND DISCUSSION</b> .....	<b>12</b>
54	3.1	OPTIMIZATION OF THE ICP OPERATING PARAMETERS .....	12
55	3.2	ANALYTICAL FIGURES OF MERIT .....	13
56	3.3	APPLICATION CASES : .....	18
57	3.3.1	Ultra trace sulfur determination in solvents using ICP-MS/MS .....	18
58	3.3.2	Trace elemental composition of Asphaltenes by ICP-MS/MS .....	19
59	3.3.3	Speciation of Ni, V and S in heavy petroleum cuts by GPC-ICP-MS .....	21
60	<b>4</b>	<b>CONCLUSIONS</b> .....	<b>26</b>
61	<b>5</b>	<b>ACKNOWLEDGMENTS</b> .....	<b>28</b>
62	<b>7</b>	<b>TABLES AND FIGURES</b> .....	<b>34</b>
63	<b>8</b>	<b>SUPPLEMENTARY MATERIAL</b> .....	<b>35</b>
64			
65			

## 66           **1 Introduction**

67 Intensive studies have been dedicated to trace and ultra trace metals determination in petroleum  
68 products in the recent years [1–4]. The need of the petroleum industry in this field is related to  
69 exploitation activities and exploration : contamination during oil production and refining (e.g.  
70 prevention of catalyst poisoning, corrosion and pollution control [5]), and geochemical  
71 characterization of source rocks and basins in order to identify geochemical biomarkers [6] in oil-  
72 oil or oil-source rock correlation. The existence of metals in fossil fuels was firstly established by  
73 Alfred Treibs in the 1930s [7]. Trace metals are also incorporated into petroleum fractions as  
74 organometallic compounds (*e.g.* geoporphyrins) initially present in the crude oil [8] or added  
75 during the various processes of refining [9]. Their concentration are always ranged between  
76  $\mu\text{g}/\text{kg}$  and  $\text{mg}/\text{kg}$  levels but low amount of certain metals can have drastic effects as a  
77 contaminant. The determination of a particular metal is mainly driven by their poisoning effect on  
78 catalysts during refining processes [10]. It is then important to better characterise their  
79 distribution in the petroleum fractions as this can improve oil refining strategies. Thus, several  
80 characterization of metal complexes in petroleum products exist and if we focus on heavy  
81 fractions and oils that are more and more used in the petrochemical industry, vanadium (V),  
82 nickel (Ni), and sulfur (S) present in these oils plays a critical role during oil-refining processes.  
83 These elements could lead to corrosion of the equipment, environmental pollution, and  
84 contamination of the final petroleum products. In order to treat them efficiently, information on  
85 the size and chemical form (speciation) of these elements are of major importance to choose the  
86 porosity of refining catalysts.

87 Many techniques have been used for the determination of metals in petroleum fractions including  
88 X-rays fluorescence (XRF) [11,12] or microwave induce plasma atomic emission spectrometry  
89 (MIP-AES) [13] or even laser induced breakdown spectroscopy (LIBS) analysis [14]. For total  
90 trace determination, inductively coupled plasma (ICP) techniques are generally used [3,4,15,16]  
91 and allow sufficient detection limits for most of the cases in the petroleum industry and are also  
92 conventionnaly hyphenated to separation techniques to reach speciation analyses [17,18]. The  
93 inherent high sensitivity of ICP-MS detection together with isotopic ratio capabilities opens new  
94 fields of applications in petrochemistry or geochemistry, but the introduction of organic  
95 substances is not that easy as this technique was not initially designed for organic samples  
96 analysis [4]. Specific configurations of sample introduction systems are required in order to

97 minimize organic solvent load into the ICP plasma [19]. Moreover, specific polyatomic  
98 interferences are disturbing the spectra due to the massive presence of carbon, oxygen and sulfur  
99 within the plasma, originating from the petroleum cuts. For this reason, various approaches have  
100 been adopted within the last years in order to minimize the presence of carbon within the plasma:  
101 emulsification, decomposition of the sample matrix, but also laser ablation and analysis through  
102 electrothermal vaporization. Most of these approaches were already reviewed in [3] and the  
103 advantages and drawbacks of the introduction of organic/hydro-organic matrices in ICP was  
104 deeply reviewed by [4,20].

105 The determination of light or interfered elements done in the specific case of direct injection of  
106 the organic substances within the plasma torch of the ICP-MS was mainly done with the help of  
107 high resolution ICP-HRMS [21,22], essentially when difficult isotopic interferences are present  
108 [23,24]. Such an instrument is quite expensive and not available in most of the lab of the  
109 petroleum industry for routine organic analyses. The recent commercialisation of an inductively  
110 coupled plasma tandem mass spectrometry (ICP-MS/MS) by Agilent [25–28] and Thermo  
111 Fischer Scientific [29], is specifically dedicated to solve polyatomic interferences in organic  
112 solvents and attain lower detection limit. It will be then interesting for the petroleum industry to  
113 investigate this instrument in order to have a specific idea of the capabilities of such system for  
114 difficult elements (for example S, Si, Fe) and especially for heavy matrices. In 2017, a complete  
115 review about ICP-MS/MS applications for total and speciation analyses was published [28].  
116 However, to our knowledge, a very few number of papers [26,30] are reported in the literature  
117 about the application of the ICP-MS/MS to organic products with direct injection, and the most  
118 difficult solvent used was ethanol. Ethanol is anyway not a sufficient “good solvent” to solubilize  
119 most of the petroleum fractions and harsher solvent (difficult to introduce in the plasma) like  
120 xylene or even THF are commonly used to dissolve hydrocarbons. In order to avoid difficult  
121 organic solvent introduction into the plasma, two recent papers reported acid digestion of  
122 petroleum products followed by ICP-MS/MS for multi elements analysis at trace levels, allowing  
123 external calibration by means of aqueous standards but this preparation step is time consuming  
124 compared to direct injection [31,32].

125 Also for the speciation of heavy crude oils a few number of papers is existing in the literature.  
126 One of the main approaches proposed actually in the literature is based on the use of gel

127 permeation chromatography (GPC) coupled to ICP-HRMS [23,24] and very recently ICP-  
128 MS/MS [33].

129 This work is based on the direct injection of hydrocarbons after solvent dilution within the  
130 plasma torch of the ICP-MS in order to minimize the preparation steps, but also to support  
131 organic solvent issued from separation techniques. This article will present the two approaches  
132 for total direct determination of organic substances and speciation with GPC obtained with an  
133 ICP-MS/MS compared to ICP-HRMS for various elements and matrices. The interferences due  
134 to the presence of carbon, oxygen and sulfur within the plasma are solved with the use of a  
135 collision/reaction chamber [18] or the use of high resolution ICP-MS [21,34]. Optimization  
136 parameters for these two configurations are optimized and the different figures of merit are  
137 discussed concerning linearity, background equivalent concentration (BEC) and detection limits.  
138 Three cases of application in the petroleum industry (Ultra trace sulfur in solvents, Asphaltene  
139 elemental composition and Speciation in heavy matrices) are then presented to give an overview  
140 of the capabilities of the ICP-MS/MS compared to the ICP-HRMS.

141

## 142           2   Materials and methods

### 143   2.1   Solutions and samples

144   Different lots of the same solvent grades of toluene and xylene (mixture of o, m, p-xylene)  
145   AnalaR Normapur were obtained from VWR Chemicals (Fontenay s/s Bois, France) and used for  
146   most of the preparation and sulfur detection. For the GPC experiments, American Chemical  
147   Society-grade THF with 250 ppm of butylated hydroxytoluene (BHT) as stabilizer (Scharlau,  
148   Spain) was used for the solutions, sample dilutions and as the mobile phase. A Premisolv solvent  
149   was provided by SCP Science (Courtabouef, France) and used as a sulfur free solvent.

150   A Conostan (SCP Science, Courtabouef, France) multi-element oil-based standards (S-21+CoK)  
151   containing 500 mg/kg of Ag, Al, B, Ba, Ca, Cd, Co, Cr, Cu, Fe, K, Mg, Mn, Mo, Na, Ni, P, Pb,  
152   Si, Sn, Ti, V and Zn was used. A specific mono-elemental oil-based standard was used for S, Hg  
153   and As calibration. Multi-element working standard solutions at 0.10, 0.20, 0.50, 1.0, 2.0, 5.0, 10,  
154   20 and 50 µg/kg, were prepared by the appropriate dilution of these solutions in xylene.  
155   Calibration solutions were prepared by weighing and the exact added concentrations were  
156   recalculated afterwards.

157   Different petroleum cuts are provided by IFP Energies nouvelles (IFPEN) (Solaize, France) and  
158   their main characteristics are described in Table 1. Straight Run Naphtha samples directly issued  
159   from different refineries were used as sulfur free solvent. Vacuum residue (VR) from Middle East  
160   already used in [24] and its hydrotreated (HDT) vacuum residue issued from a deep  
161   hydrodemetallation pilot plant experiment (E) were used for GPC analyses. Asphaltenes fraction  
162   (A) was recovered from the partial Vacuum residue flocculation in contact with the n-heptane as  
163   already described in [35].

164

165

166

167

168

169



170 **Table 1: Characteristics of the petroleum cuts provided for the various experiments.**

Samples	Simulated distillation IFPEN 1202			XRF		
	T5	T50	T95	Ni [mg/kg]	V [mg/kg]	S [%w/w]
Asphaltene A	na	na	na	350	655	na
Naphtha 16J	15	88.7	158	na	na	na
Naphtha 16F	49	100	185	na	na	na
Naphtha 16A	24	71	145	na	na	na
Vacuum Residue VR	482	625	725	58	183	5.7
HDT vacuum residue E	na	na	na	3	6	0.49

171 na: not available

## 172 **2.2 Instrumentation**

### 173 *2.2.1 ICP-MS and GPC-ICP-MS*

174 ICP-MS and GPC-ICP-MS analyses were achieved using an ICP-MS/MS and a ICP-HRMS. The  
 175 most important instrumental parameters are presented in Table 2. The first one is an ICP-MS/MS  
 176 8800 instrument from Agilent (Agilent Technologies, Japan). In this instrument, the collision-  
 177 reaction cell (CRC) is an octopole located in-between two quadrupole analyzers, this cell can be  
 178 filled with a collision or a reactive gas in order to reduce interferences on the ions of interest. All  
 179 monitored isotopes are detailed in Table 2 in function of the resolution (low, medium, high) for  
 180 the ICP-HRMS and gas mode (no gas, He, H<sub>2</sub> and O<sub>2</sub> mode) for the ICP-MS/MS. In No gas  
 181 mode, the width of the bandpass of the first quadrupole analyzer is fully open or used as an ion  
 182 guide and the second quadrupole analyzer is set at the chosen mass. In He gas mode, the width of  
 183 the bandpass of the first quadrupole analyzer is fully open and the second quadrupole analyzer is  
 184 set at the chosen mass. In H<sub>2</sub> gas mode, the width of the bandpass of the first quadrupole analyzer  
 185 is set to single mass width and the second quadrupole analyzer is set to the same single mass  
 186 width because H<sub>2</sub> did not react with the chosen elements. Finally for the O<sub>2</sub> gas mode, the width  
 187 of the bandpass of the first quadrupole analyzer is set to the element of interest mass width and  
 188 the second quadrupole analyzer is set to the element of interest mass width + 16 to let the  
 189 monoxide of the element going through the second quadrupole: For some elements in the oxygen

190 mode, the mass of the second quadrupole is let to the same single mass width in order to verify  
191 the reactivity of the element and how much has not reacted within the collision/reaction chamber.  
192 This was the case for :  $^{48\rightarrow 48}\text{Ti}$ ,  $^{51\rightarrow 51}\text{V}$ ,  $^{56\rightarrow 56}\text{Fe}$ ,  $^{59\rightarrow 59}\text{Co}$ ,  $^{60\rightarrow 60}\text{Ni}$ ,  $^{62\rightarrow 62}\text{Ni}$ ,  $^{75\rightarrow 75}\text{As}$ .  
193 The second ICP-MS is an Element XR double focusing sector field inductively coupled plasma  
194 mass spectrometer (Thermo Fisher, Germany). A micro-flow total consumption nebulizer (DS-1,  
195 Cetac) without drain [36] was tested. Samples were delivered using an ASX-520 (CETAC,  
196 Omaha, NE) autosampler. Some elements were monitored with low resolution ( $R=300$ ), medium  
197 resolution ( $R=4000$ ) and high resolution mode ( $R=10000$ ). Samples were delivered using an  
198 ASX-500 (CETAC, Omaha, NE). For total experiments, the reduction of the amount of organic  
199 vapor entering the plasma was obtained using a Peltier-cooled spray chamber cooled down at  $-5$   
200  $^{\circ}\text{C}$ .  
201 For both instruments, the sampler and skimmer cones covered with Pt were used due to organic  
202 injection and the necessity of adding oxygen within the plasma.  
203 For the GPC experiment, the mobile phase was delivered by a Dionex HPLC system with an  
204 UltiMate 3000 microflow pump, an UltiMate 3000 autosampler, and a low port-to-port dead-  
205 volume microinjection valve. Chromatographic separation was performed by three polystyrene-  
206 divinylbenzene GPC columns connected in series (porosity of  $100 \text{ \AA}$ ,  $1000 \text{ \AA}$  and  $10,000 \text{ \AA}$ ). The  
207 GPC eluted fractions were splited to introduce the same flow of  $0.03 \text{ ml/min}$  as total analysis  
208 (Table 2) into the high resolution ICP-MS *via* a modified DS-5 microflow total consumption  
209 nebulizer (CETAC, Omaha, NE) fitted with a laboratory-made single-pass glass spray chamber  
210 thermostated at  $60 \text{ }^{\circ}\text{C}$  by a water/glycol mixture using a temperature controlled bath circulator  
211 (Neslab RTE-111, Thermo Fisher Scientific, Waltham, MA).  
212 The same set of columns was used with the Agilent 8800 ICP-MS instrument. An Agilent 1290  
213 Infinity liquid chromatographic device was used. The elution system was equipped by specific  
214 THF resistant parts. In this case, the total GPC eluted fractions was introduced within the Scott  
215 spray chamber by the means of a Burgener T2002 nebulizer using Pharmed tubing.  
216 To minimize carbon-buildup on the sampler cone,  $\text{O}_2$  was added within a mixture of  
217 Argon/oxygen ( $\text{Ar}/\text{O}_2:80/20$ ) between the spray chamber and the torch for the ICP-MS/MS, a  
218 typical flow between  $230$  and  $270 \text{ mL/min}$  of the  $\text{Ar}/\text{O}_2$  mixture is used depending on the  
219 application. Pure oxygen was added to the sample Ar flow using a mass flow controller with the  
220 ICP-HRMS, a flow of  $80 \text{ mL/min}$  was used.

221 **Table 2: Operating conditions for total analysis using ICP-MS apparatus**

	ThermoFisher Element HRMS with DS-1	Agilent ICP-MS/MS 8800
RF power [W]	1500	1550
Plasma gas flow [L/min]	16	18
Optional gas flow [L/min]	O <sub>2</sub> : 0.08	Ar+O <sub>2</sub> : 0.23-0.27*
Carrier gas flow [L/min]	0.565	0.50
Auxiliary gas flow rate [L/min]	0.9	
Number of replicates	3	3
Liquid flow rate [ml/min]	0.03	0.50-0.70*
Nebulizer	Modified DS-5	Burgener T2002
Nebulization chamber	Low dead volume (8 cm <sup>3</sup> ) spray chamber without drain [36]	Scott type – double pass
Spray chamber temperature [°C]	60	-5
Torch Z-position [mm]	-3	5
Injector	1.0 mm ID quartz injector	1.0 or 1.5 mm ID quartz injector
Detection mode	Triple	
Resolution (HRMS) and gas mode (ICP-MS/MS) for monitored elements	<p>-low resolution (R=3000)  <sup>10</sup>B, <sup>11</sup>B, <sup>23</sup>Na, <sup>27</sup>Al, <sup>29</sup>Si, <sup>31</sup>P, <sup>34</sup>S, <sup>44</sup>Ca, <sup>46</sup> and <sup>47</sup>Ti, <sup>51</sup>V, <sup>53</sup>Cr, <sup>54</sup>Fe, <sup>59</sup>Co, <sup>60</sup>Ni, <sup>63</sup> and <sup>65</sup>Cu, <sup>66</sup> and <sup>68</sup>Zn, <sup>75</sup>As, <sup>95</sup> and <sup>98</sup>Mo, <sup>107</sup> and <sup>109</sup>Ag, <sup>118</sup> and <sup>120</sup>Sn, <sup>137</sup> and <sup>138</sup>Ba, <sup>200</sup> and <sup>202</sup>Hg, <sup>206</sup>, <sup>207</sup> and <sup>208</sup>Pb</p> <p>-medium resolution (R=4000)  <sup>10</sup> and <sup>11</sup>B, <sup>23</sup>Na, <sup>27</sup>Al, <sup>28</sup> and <sup>29</sup>Si, <sup>31</sup>P, <sup>32</sup> and <sup>34</sup>S, <sup>39</sup>K, <sup>44</sup>Ca, <sup>46</sup> and <sup>48</sup>Ti, <sup>51</sup>V, <sup>52</sup> and <sup>53</sup>Cr, <sup>54</sup> and <sup>56</sup>Fe, <sup>59</sup>Co, <sup>58</sup> and <sup>60</sup>Ni, <sup>63</sup> and <sup>65</sup>Cu, <sup>75</sup>As, <sup>95</sup> and <sup>98</sup>Mo, <sup>107</sup> and <sup>109</sup>Ag, <sup>118</sup> and <sup>120</sup>Sn, <sup>137</sup> and <sup>138</sup>Ba, <sup>200</sup> and <sup>202</sup>Hg, <sup>206</sup>, <sup>207</sup> and <sup>208</sup>Pb</p> <p>-high resolution (R=10000)  <sup>28</sup>Si, <sup>39</sup>K and <sup>75</sup>As</p>	<p>-No gas  <sup>10</sup>B, <sup>11</sup>B, <sup>23</sup>Na, <sup>34</sup>S, <sup>51</sup>V, <sup>58</sup>Ni, <sup>59</sup>Co, <sup>60</sup>Ni, <sup>62</sup>Ni, <sup>63</sup>Cu, <sup>65</sup>Cu, <sup>66</sup>Zn, <sup>75</sup>As, <sup>95</sup>Mo, <sup>97</sup>Mo, <sup>107</sup>Ag, <sup>109</sup>Ag, <sup>118</sup>Sn, <sup>120</sup>Sn, <sup>135</sup>Ba, <sup>137</sup>Ba, <sup>200</sup>Hg, <sup>201</sup>Hg, <sup>202</sup>Hg, <sup>206</sup>Pb, <sup>207</sup>Pb, <sup>208</sup>Pb</p> <p>-He mode  <sup>23</sup>Na, <sup>27</sup>Al, <sup>31</sup>P, <sup>47</sup>Ti, <sup>49</sup>Ti, <sup>51</sup>V, <sup>52</sup>Cr, <sup>53</sup>Cr, <sup>56</sup>Fe, <sup>57</sup>Fe, <sup>58</sup>Ni, <sup>59</sup>Co, <sup>60</sup>Ni, <sup>62</sup>Ni, <sup>63</sup>Cu, <sup>65</sup>Cu, <sup>66</sup>Zn, <sup>68</sup>Zn, <sup>75</sup>As</p> <p>-H<sub>2</sub> mode  <sup>27</sup> &gt; <sup>27</sup>Al, <sup>28</sup> &gt; <sup>28</sup>Si, <sup>51</sup> &gt; <sup>51</sup>V, <sup>52</sup> &gt; <sup>52</sup>Cr, <sup>53</sup> &gt; <sup>53</sup>Cr, <sup>56</sup> &gt; <sup>56</sup>Fe, <sup>57</sup> &gt; <sup>57</sup>Fe, <sup>58</sup> &gt; <sup>58</sup>Ni, <sup>59</sup> &gt; <sup>59</sup>Co, <sup>60</sup> &gt; <sup>60</sup>Ni, <sup>62</sup> &gt; <sup>62</sup>Ni, <sup>63</sup> &gt; <sup>63</sup>Cu, <sup>65</sup> &gt; <sup>65</sup>Cu, <sup>66</sup> &gt; <sup>66</sup>Zn, <sup>68</sup> &gt; <sup>68</sup>Zn</p> <p>-O<sub>2</sub> mode  <sup>31</sup> &gt; <sup>47</sup>P, <sup>32</sup> &gt; <sup>48</sup>S, <sup>33</sup> &gt; <sup>49</sup>S, <sup>34</sup> &gt; <sup>50</sup>S, <sup>48</sup> &gt; <sup>64</sup>Ti, <sup>51</sup> &gt; <sup>67</sup>V, <sup>56</sup> &gt; <sup>72</sup>Fe, <sup>58</sup> &gt; <sup>74</sup>Ni, <sup>60</sup> &gt; <sup>76</sup>Ni, <sup>62</sup> &gt; <sup>78</sup>Ni, <sup>75</sup> &gt; <sup>91</sup>As</p> <p><sup>48</sup> &gt; <sup>48</sup>Ti, <sup>51</sup> &gt; <sup>51</sup>V, <sup>56</sup> &gt; <sup>56</sup>Fe, <sup>59</sup> &gt; <sup>59</sup>Co, <sup>60</sup> &gt; <sup>60</sup>Ni, <sup>62</sup> &gt; <sup>62</sup>Ni, <sup>75</sup> &gt; <sup>75</sup>As, <sup>58</sup> &gt; <sup>58</sup>Ni</p>
Extract [V]	-2000	1: 0 - 2: -160
Omega bias [V]		-80
Cell gas		no gas/ O <sub>2</sub> (0.23-0.32 mL/min)/ He (2-3 mL/min)/ H <sub>2</sub> (2-3.1 mL/min)

222 \*For GPC, different liquid and Ar+O<sub>2</sub> flow rates are used after optimization

223            2.2.2 *UVF and XRF apparatus*

224 UVF analysis following ISO 20486 was performed using an Antek Multitek (PAC-Alytech,  
225 Juvisy sur Orge, France) with syringe injection. The instrument was calibrated between 0.2 and 2  
226 mg/kg with DiButylSulfide and a volume of 20  $\mu$ L was injected.

227 For wavelength dispersive X-rays fluorescence (WDXRF) analysis, a Panalytical Axios (Almelo,  
228 Netherlands ) 4 kW equipped with a Cr anode was used. 6 ml of the solution was introduced  
229 within a cup with a Mylar 6 $\mu$ m film. The Ni and V  $K_{\alpha}$  were followed and the C/H and S matrix  
230 effect were compensated using the Cr Compton line according to an internal IFPEN method.

231

232           **3 Results and discussion**

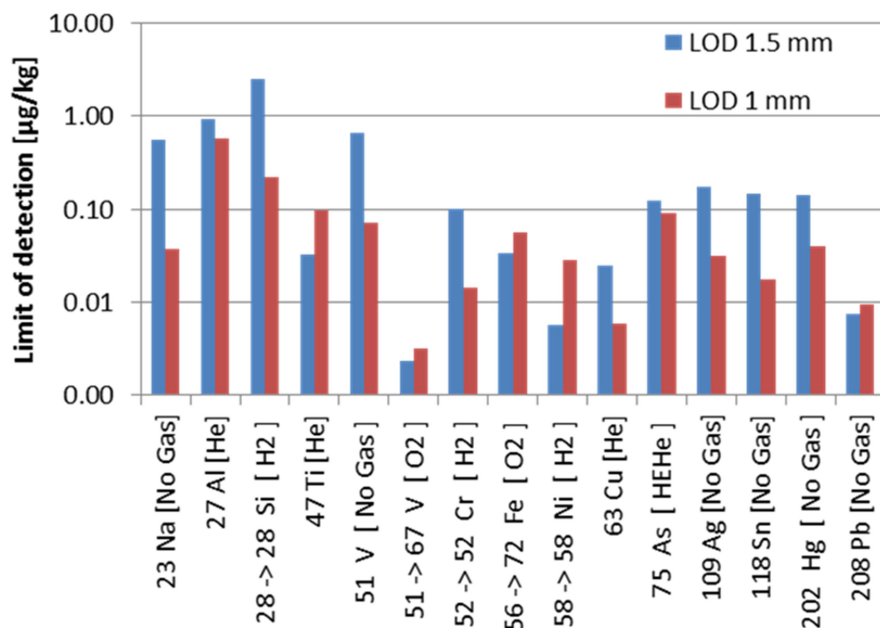
233    **3.1 Optimization of the ICP operating parameters**

234    The configuration of the ICP-MS/MS and the ICP-HRMS was tested by calibrating the  
235    instruments between 0 to 50 or 100 µg/kg in xylene. Polyatomic interferences were solved by the  
236    use of medium resolution (R=4000) with the HRMS or with the use of the a collision/reaction  
237    cell using the ICP-MS/MS. For the different gas modes used with the ICP-MS/MS, the carrier  
238    gas was firstly optimized and then the various lenses were adjusted. The gas flow in the  
239    collision/reaction was finally optimized according to each application tested in order to reach the  
240    best signal to noise ratio.

241    Most of the optimized parameters both for the ICP-MS/MS and the ICP-HRMS are reported in  
242    Table 2. According to Agilent recommendations for organic introduction, the standard injector  
243    tube (2.5 mm internal diameter) was replaced by a 1.5 mm i.d. injector. Two types of injector  
244    were tested with the 1.5 and 1.0 mm internal diameter. The two configurations tested shows that  
245    for most of the elements the 1.0 mm injector allowed similar detection limit or increase of the  
246    sensitivity by a factor up to 10 times. This increase of sensitivity was more effective for lighter  
247    elements with atomic mass lower than 30 (Figure 1). The 1.0 mm injector was then kept for each  
248    application, as previously reported by Poirier *et al.*, [15] for the total analysis of Ni, V, Fe and Ca  
249    in petroleum crude oil *via* direct dilution using ICP-MS.

250

251



252

253 **Figure 1: Comparison of detection limits obtained using diameters 1.0 and 1.5 mm for two injectors**  
 254 **proposed for the ICP-MS/MS.**

255 **3.2 Analytical figures of merit**

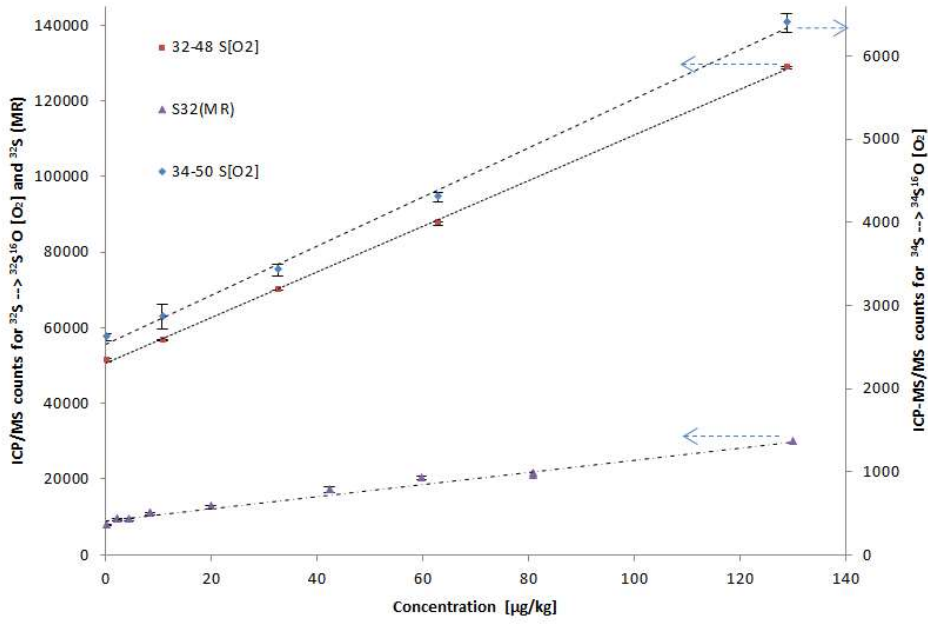
256 For each element, the calibration curve was built acquiring the signal for various isotopes and  
 257 using the diversity of the modes offered by each instrument. Low, medium and high resolutions  
 258 were followed with the ICP-HRMS and the no gas, helium, hydrogen and oxygen modes were  
 259 used and optimized with the ICP-MS/MS. Typical curves for heavy interfered elements (S, Si,  
 260 Fe) are respectively shown Figure 2 to Figure 4 for the most sensible mode retained for each  
 261 element. From each calibration curve, the limit of detection (LOD) and the background  
 262 equivalent concentration (BEC) are calculated according to the following equation:

263

264  $y = ax + b$  with  $BEC = b/a$  and  $LOD = 3xBECxRSD_{blk}$  [37]

265 The relative standard deviation of the blank ( $RSD_{blk}$ ) was calculated according to 3 replicates of  
 266 xylene.

267

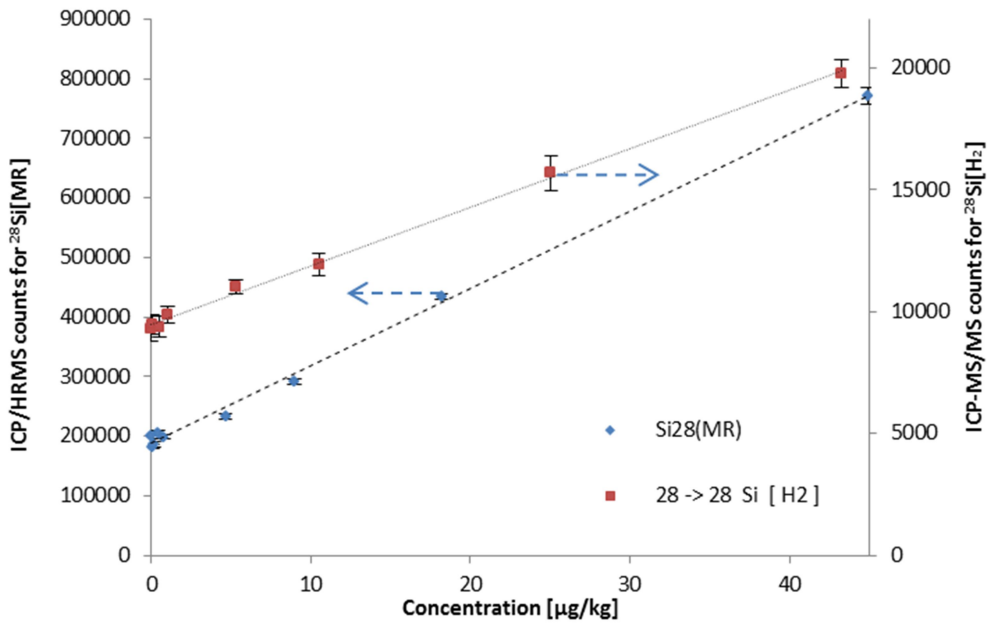


268

269 **Figure 2: Calibration curves for S using ICP-HRMS or ICP-MS/MS (Arrows indicate the correct**  
 270 **axis for all calibration curves)**

271

272

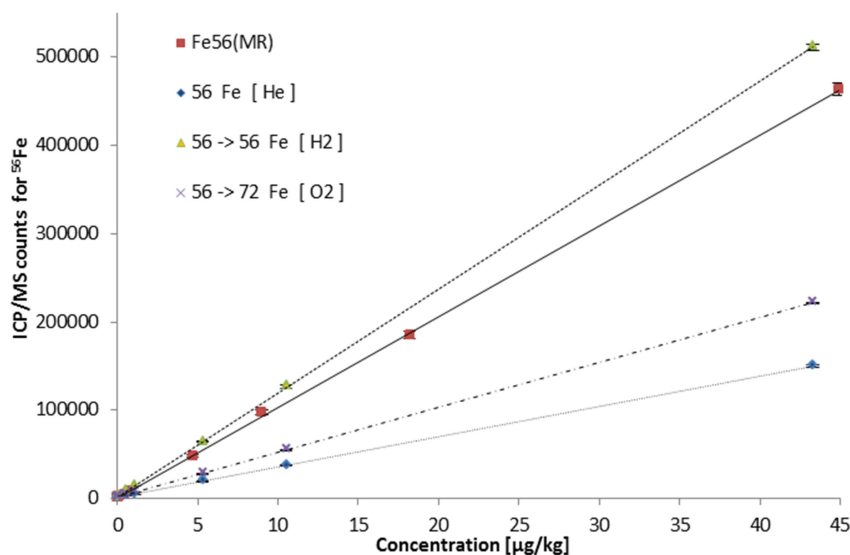


273

274 **Figure 3: Calibration curves for Si using ICP-HRMS or ICP-MS/MS (Arrows indicate the correct**  
275 **axis for all calibration curves)**

276

277



278

279 **Figure 4: Calibration curves for Fe using ICP-HRMS or ICP-MS/MS**

280

281 For S, Si, and Fe, respectively presented in Figure 2, Figure 3 and Figure 4, a nice sensitivity is  
282 obtained allowing trace elemental analysis in organic products. Anyhow, the BEC for S and Si is  
283 rather high compared to Fe. This high BEC might be due to contamination of the solvent or  
284 background emission not resolved by the high resolution or configuration of the ICP-MS/MS. For  
285 S, the origin of this BEC will be discussed later in 3.3.1, but for Si this phenomenon was already  
286 observed in Chainet *et al.* [18] and was attributed to the use of an injector and torch made of  
287 quartz that provoke a Si background signal.

288 The results obtained for most of the elements for both the ICP-HRMS and the ICP-MS/MS are  
289 represented in Figure 5. For light elements ( $Z < 40$ ) having no specific interferences, the new ICP-  
290 MS/MS has better or similar performances than the ICP-HRMS. For heavy elements ( $Z > 70$ ), the  
291 ICP-MS/MS is a little bit less sensible than the ICP-HRMS due to a better transmission of ions  
292 through the magnetic and electrostatic sectors in the low resolution mode. This is also due to the  
293 fact that these elements do not suffer from interferences and that the low-resolution mode is

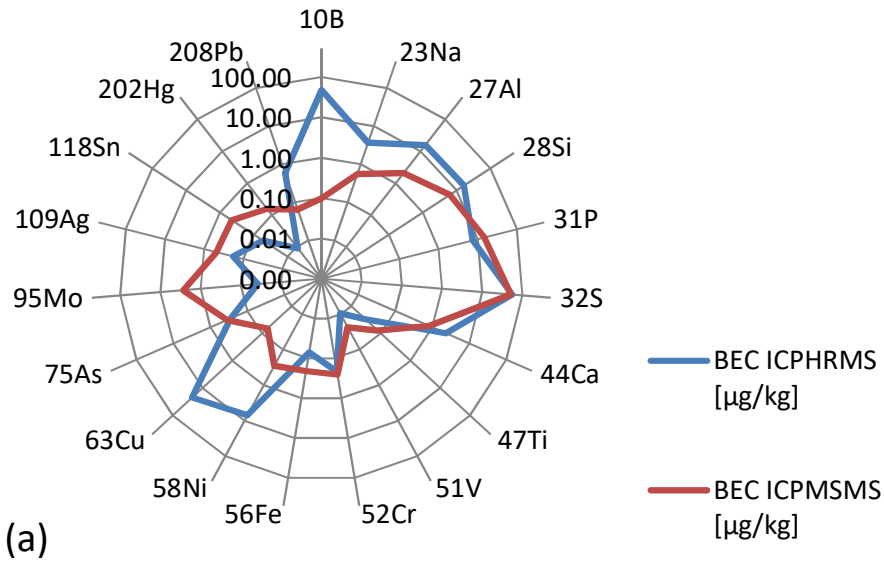


294 sufficient to transmit these isotopes to the detector. For more difficult elements having  
295 interferences, the potential of the ICP-MS/MS with different gases (H<sub>2</sub>, He, O<sub>2</sub>) and the use of the  
296 initial quad to limit the analyte entering the reaction chamber allows similar or better  
297 performances than the ICP-HRMS using medium resolution. Important elements for the  
298 petroleum industry (S, Si, Fe), but also for new biofuels specifications (P, Ca) have excellent  
299 performances compared to conventional system using traditional single quadrupole ICP-MS.

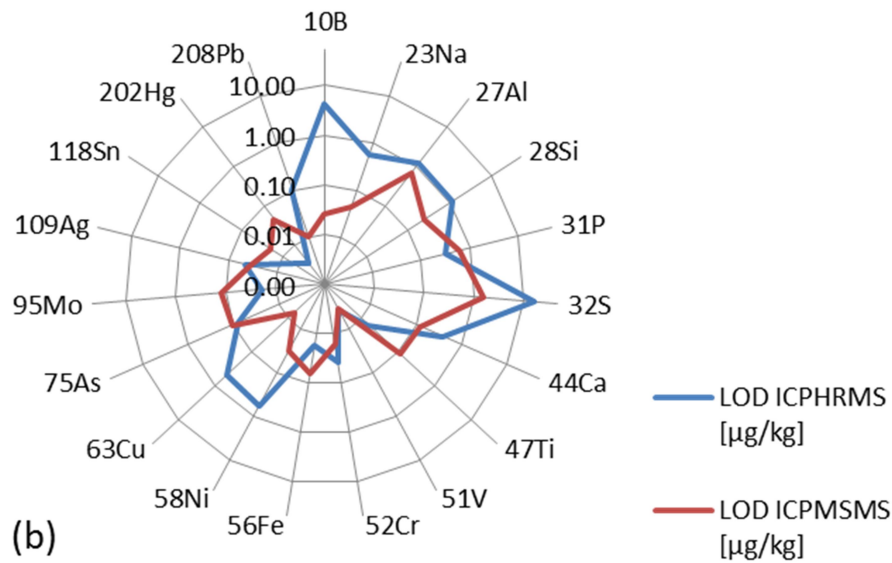
300

301

302



303



304

305 **Figure 5: Comparison of Background Equivalent Concentration (a) and Limit of Detection (b) for**  
 306 **various elements between ICP-HRMS and ICP-MS/MS detection.**

307

### 308 3.3 Application cases :

#### 309 3.3.1 Ultra trace sulfur determination in solvents using ICP-MS/MS

310 The sulfur determination in petroleum products is not a real challenge as most of products are  
311 containing more than traces level of sulfur. There is however some cases where the sulfur  
312 concentration might be challenging, typically for naphtha used in reforming application where the  
313 concentration of sulfur might be as low as possible. When the calibration for sulfur is done at low  
314 level (Figure 2), the BEC is important compared to the LOD obtained for such element (Figure 5)  
315 and this was already pointed by preceding work [26]. Anyhow, most of the work done until now  
316 for S in organic matrices with ICP-MS/MS are using isotopic dilution after digestion procedure  
317 [27,30–32] and measure S levels between 4 mg/kg and 2.7%.

318 For very low levels of S, it was then important to determine the origin of this BEC, considering  
319 that different sources of BEC can be attributed. Typically, the BEC can be due to solvent  
320 contamination ( $BEC_{\text{solvent}}$ ) or noise due to the instrumentation contamination or electronic noise  
321 of the detection. ( $BEC_{\text{instrumental}}$ ). It should be noted that using digestion procedures, Yang *et al.*  
322 [32] observe a very low BEC in aqueous matrices.

323 Four different solvents (toluene, xylene, naphtha, Premisolv) were then tested to determine the  
324 various contributions of the BEC with different lot numbers and volatility. For this experiment, a  
325 calibration curve was prepared with adding of S using a sulfur mono-elemental oil-based standard  
326 between 5 and 300  $\mu\text{g}/\text{kg}$  in the four selected solvents. These mixtures were introduced into the  
327 ICP-MS/MS and the settings of the plasma were adjusted in order to have the best signal to noise  
328 ratio of the instrument depending on the volatility of the solvent injected. One condition per  
329 solvent were retained and the  $^{32}\text{S} \rightarrow ^{48}\text{S}$  and  $^{34}\text{S} \rightarrow ^{50}\text{S}$  transition were kept to measure the S signal  
330 within each solvent. The  $^{34}\text{S}/^{32}\text{S}$  isotope ratio of the S signal within the different solvents is  
331 interesting with a value of  $21.20 \pm 0.83$ . This value is very similar to the theoretical value of 22.5  
332 for the relative abundance of naturally S occurring isotope and this concordance might confirm  
333 that the BEC of the instrument is mainly driven by the S signal and not due to electronic noise.

334 The BEC obtained for each solvent and conditions is given in Table 3. The BEC is not equivalent  
335 when different lots of the same solvent are analyzed. As the conditions of the plasma was linked  
336 to the use of specific solvent and different BEC were obtained with an unique condition of the  
337 plasma, this difference of the BEC can then be attributed to the lot number of the solvent and then

338 directly to its residual S concentration. This indicates that the residual S concentration present in  
 339 the solvent might be the only contributor to the BEC and that the  $BEC_{\text{instrumental}}$  might be  
 340 negligible. The Premisolv was also analyzed by UVF following ISO 20846 due to its high level  
 341 of sulfur. A comparative value of 233  $\mu\text{g}/\text{kg}$  was obtained with this technique, showing that the  
 342 level of the BEC with the ICP-MS/MS (251  $\mu\text{g}/\text{kg}$ ) is mainly due to the S contamination. The  
 343 BEC obtained for each new solvent can then be assigned to the level of concentration of sulfur in  
 344 the solvent as it is conventionally done when standard addition are used. It is then possible to  
 345 measure ppb level of S in various solvents by spiking the solvent with increasing concentrations  
 346 of S and determining the S content by standard addition. It is interesting to note that pollution  
 347 between 30 to 250  $\mu\text{g}/\text{kg}$  of S were observed in the various solvents used in this work. Such  
 348 information might be crucial for selecting feed used in reforming application.

349 **Table 3: BEC [ $\mu\text{g}/\text{kg}$ ] of  $^{32\rightarrow 48}\text{S}$  obtained for each solvent and plasma conditions.**

Lot number \ Solvents:	Naphtha	Toluene	Xylene	Premisolv
16J	75		78	
16F	86	80	32	
15G			54	
16A	68	98		
others				251

350 *3.3.2 Trace elemental composition of Asphaltenes by ICP-MS/MS*

351 Asphaltenes fraction are known to contain an important concentration of Ni, V and S that are  
 352 easily measured due to their high level, but the minor traces are barely investigated and it might  
 353 be interesting to evaluate if others metals are present in the asphaltenes fractions of some crude  
 354 oil. In order to evaluate the feasibility of such determination, a multi-element oil-based standard  
 355 (S-21+CoK) was used to calibrate the instrument in THF between 0 to 100  $\mu\text{g}/\text{kg}$ . The conditions  
 356 of nebulization and each mode of gas ( $\text{H}_2$ , He and  $\text{O}_2$ ) were optimized due to the fact that the  
 357 volatility of THF is different than xylene previously used in section 2.2.1. Higher flow of oxygen  
 358 (0.27 compared to 0.20 mL/min), hydrogen (3.1 compared to 2.0 mL/min) and He (3.5 compared  
 359 to 2.5 mL/min) was observed for the optimum signals in the gas cell, as it was the case for the

360 optional gas (0.31 compared to 0.20 L/min). The asphaltene fraction was diluted between 700 to  
361 85000 times in THF and measured subsequently. Yttrium was added to all solutions to verify the  
362 potential impact of the viscosity of the solution and controlling the efficiency of the nebulizer  
363 with the asphaltene solution. The sulfur concentration was not measured due to the presence of  
364 sulfonates in the initial multi-element standard solution, but also the high concentration of such  
365 element that is not needing trace analysis instrument. The same fraction of asphaltene was diluted  
366 in toluene and measured by WDXRF using an internal method to measure S, Ni and V  
367 concentrations of the prepared solution. The results obtained for many elements are given in  
368 Table 4. Concentrations obtained for Ni (380 mg/kg) and V (630 mg/kg) by ICP-MS/MS are  
369 quite comparable to the conventional WDXRF IFPEN method (322 mg/kg for Ni and 655 mg/kg  
370 for V) and allow to validate the analysis of the asphaltene. As already described in the literature  
371 [38], iron is the fourth element present in the asphaltene fraction in terms of concentration. The  
372 value obtained for Mo is also very similar to others values available in the literature [16,39]. The  
373 others elements are in the same order of magnitude with value observed in the literature between  
374 sub ppm level to tenth of ppm [16,39]. Amongst them, the value for tin is quite high and might be  
375 due to container contamination.

376  
377  
378  
379  
380  
381  
382  
383  
384  
385  
386  
387  
388  
389

390 **Table 4: Concentration obtained by WDXRF and ICP-MS/MS for the asphaltene fraction**

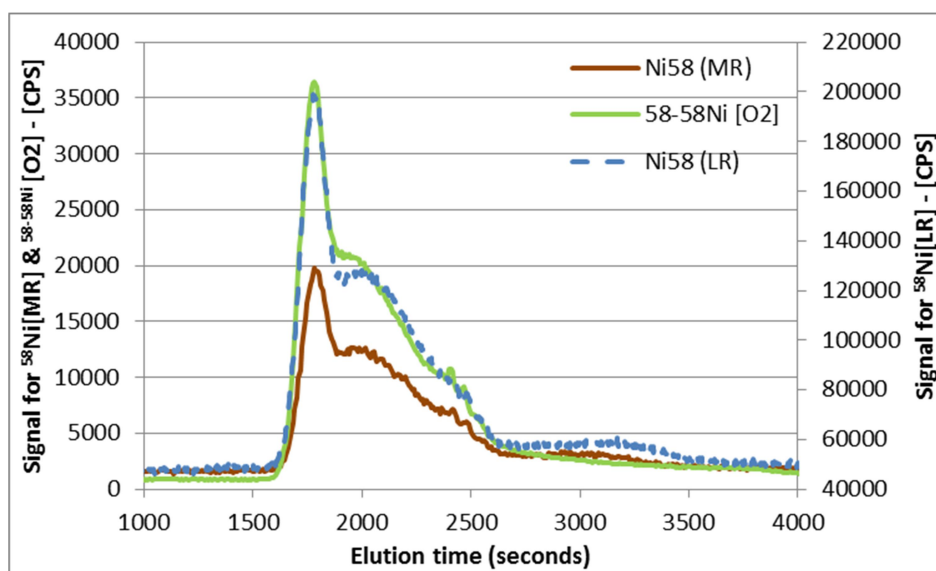
Elements	Concentration [mg/kg]	
	WDXRF	ICP-MS/MS
V	655	630
Ni	322	380
S (%)	6.87	nm
Fe	nm	37.4
Sn	nm	25
Mo	nm	8.8
Zn	nm	6.4
K	nm	4.2
Si	nm	3.9
Cr	nm	3.3
Ag	nm	1.7
Co	nm	1.6
Ba	nm	1.3
Cu	nm	1.2
Ti	nm	0.8
Pb	nm	0.3
Al	nm	0.3

391 nm : not measured

392 *3.3.3 Speciation of Ni, V and S in heavy petroleum cuts by GPC-ICP-MS*

393 Based on the excellent performance of the ICP-MS/MS for the sensitivity obtained for the  
 394 calibration curve (Section 3.2), it was then interesting to investigate the response of the  
 395 instrument when it was coupled to liquid chromatography and more specifically to GPC. Such  
 396 technique is used since years to investigate the size of Ni, V and S in various petroleum cuts, but  
 397 all of these publications are based on the use of GPC coupled to ICP-HRMS [23,24]. The  
 398 challenge to follow transient signal is the need of numerous points per peak in order to avoid loss  
 399 of resolution in the chromatogram. A very recent article mentioned the use of ICP-MS/MS to

400 monitor elemental signature on liquid chromatography [33]. Previous assay done in this work  
 401 (section 3.1) have shown that different gas modes might be necessary to have the best sensitivity  
 402 and previous work done with the ICP-HRMS have shown the use of different resolution  
 403 according to the measured element. Switching between two gas mode require 10 seconds at least  
 404 with the ICP-MS/MS and such switch is not feasible when the instrument is coupled to a  
 405 separation technique. The change of mode between high and medium resolution for ICP-HRMS  
 406 is also not described in the literature but require at least few seconds of stabilization.  
 407 Consequently, it is not compatible with the monitoring of chromatograms. It was then important  
 408 to investigate which mode of gas was the most adequate to monitor Ni, V and S during the same  
 409 acquisition. For the ICP-HRMS, previous work have shown that S is detected using medium  
 410 resolution only in order to solve the interference on the mass 32. Such higher resolution is also  
 411 reducing the intensity of the final signal due to a lower slit in front of the magnetic sector and  
 412 might be a limitation for trace element analysis. This is illustrated by the 10 times difference of  
 413 signal for Ni between low and medium resolution in Figure 6. Then for low concentration ( $< 5$   
 414 mg/kg  $Ni_{total}$ ), two injections are necessary in order to acquire V and S with the medium  
 415 resolution and Ni and V with low resolution. Such choice has an important impact on the sample  
 416 throughput due to the time of the analysis (120 minutes of run for GPC [24]).



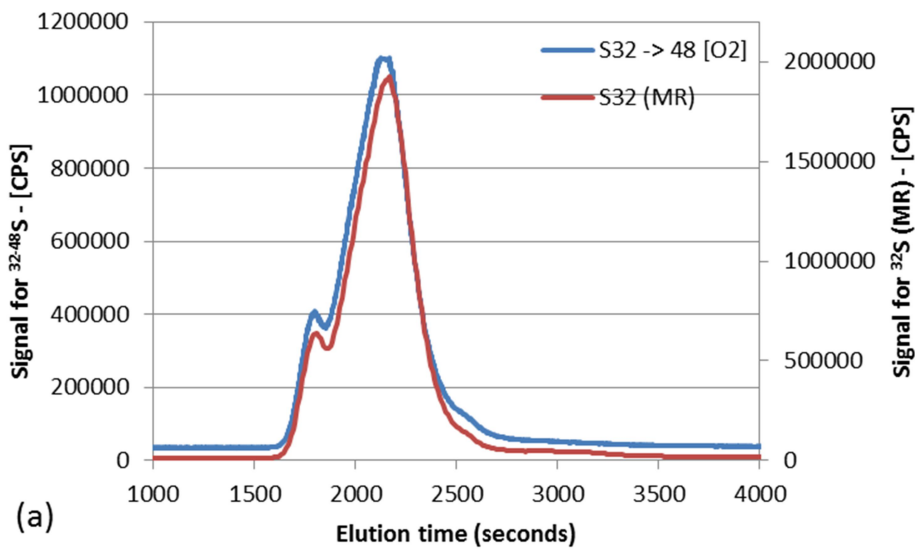
417  
 418 **Figure 6: Comparison of GPC-ICP-MS/MS and GPC-ICP-HRMS chromatograms for Ni, injecting**  
 419 **a VR with Ni content around 60 mg/kg**

420

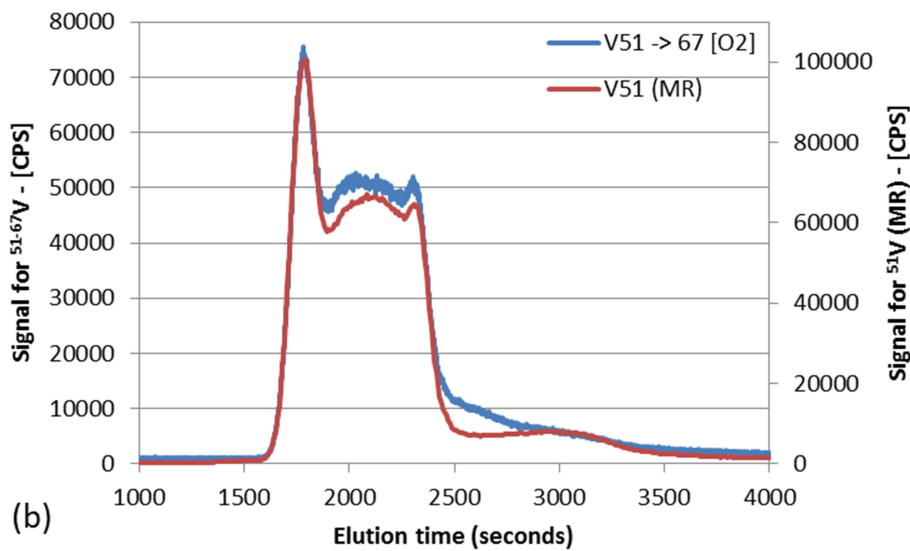
421 For the ICP-MS/MS, the O<sub>2</sub> mode was quite efficient for S (Figure 2) and V (Figure 1 and Figure  
422 S 1), but less effective for Ni due to the high enthalpy of reaction of Ni with oxygen. The He or  
423 H<sub>2</sub> mode was quite sensitive and was initially retained in the total injection (Figure 1) leading to  
424 lower sample throughput as in the case of ICP-HRMS for low concentration. Another way to  
425 observe an element with the ICP-MS/MS is to provoke a reaction within the reaction/collision  
426 cell and selecting the isotope that has not reacted at the end of the chamber. This is an interesting  
427 way to understand what has happened between the two quadrupole and is useful to understand  
428 and optimize the various instrumental conditions. Interestingly, the amount of Ni going through  
429 the reaction/collision chamber without reacting with oxygen was quite important and sufficient  
430 signal was obtained by looking at the <sup>58→58</sup>Ni [O<sub>2</sub>] mode.

431 A vacuum residue (VR) and its hydrotreated fraction (E) were eluted on the GPC column and the  
432 chromatogram obtained with the different modes are presented Figure 7 and Figure 8. The use of  
433 O<sub>2</sub> (2.5 mL/min) with Ni, V, S is particularly interesting for transient signal and allow the  
434 monitoring of the 3 elements in one mode only for the vacuum residue. For S and V (Figure 7),  
435 the signal is pretty similar for both instrument using the oxygen mode and the medium resolution  
436 but the signal to background ratio is slightly (+10%) better for the ICP-HRMS. For the Ni  
437 detection, the situation is different depending on the concentration observed on the GPC  
438 chromatogram. The profile obtained for the VR (Figure 6) is sufficient for all the mode tested.  
439 The signal to noise ratio is multiplied by a factor of two between the low and medium resolution  
440 mode of the ICP-HRMS, but the oxygen mode is even better for the ICP-MS/MS detection.  
441 When the hydrotreated feed is observed (Figure 8), the medium resolution is not sensible enough  
442 to obtain a clear distribution of the Ni entities and the use of a low resolution mode is then  
443 compulsory. This imply the use of both the medium resolution for S and V and the low resolution  
444 for Ni in order to obtain the information for all elements, reducing the sample throughput. The  
445 use of the ICP-MS/MS in the oxygen mode is sensitive enough to get a nice profile of the Ni  
446 entities on the hydrotreated feed. Such mode is then adequate to have Ni, V and S information  
447 during the same run allowing to reduce the analysis cost and time.





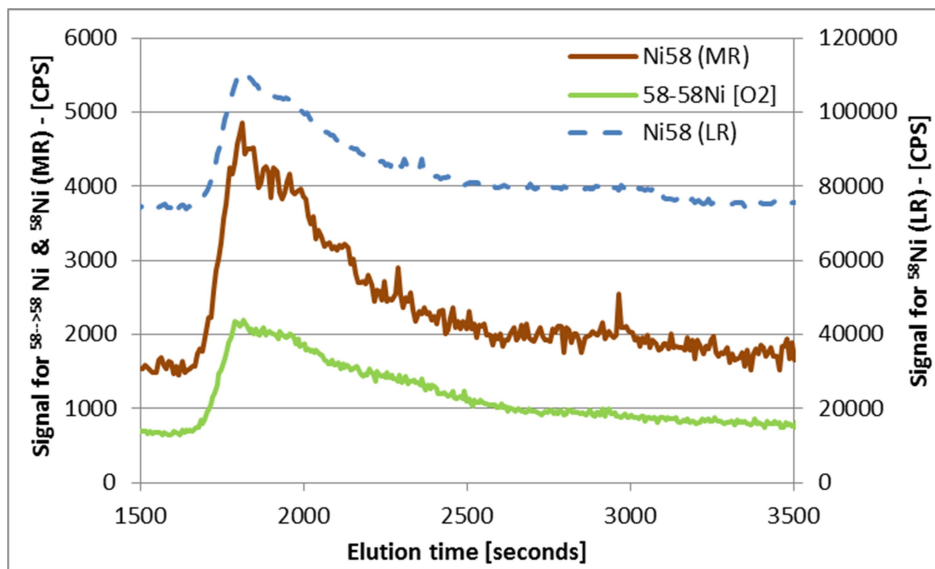
448



449

450 **Figure 7: Comparison of GPC-ICP-MS/MS and GPC-ICP-HRMS chromatograms for S (a) and V**  
 451 **(b)**

452



453

454 **Figure 8: Comparison of GPC-ICP-MS/MS and GPC-ICP-HRMS chromatograms for Ni, injecting**  
 455 **the HDT VR with Ni content around 3 mg/kg**

456

#### 4 Conclusions

457  
458 The recent inductively coupled plasma tandem mass spectrometry (ICP-MS/MS) was tested  
459 using direct injection of hydrocarbons after solvent dilution in order to investigate its use for the  
460 petroleum industry. Based on the fact that many previous authors have used ICP-HRMS for the  
461 monitoring of difficult elements in organic matrices, the results obtained for both ICP-MS/MS  
462 and ICP-HRMS were compared for both total concentration and speciation of severely interfered  
463 isotopes in petroleum products. The capability of ICP-MS/MS to achieve such performance using  
464 direct injection of petroleum products after dilution in hydrocarbon solvent was demonstrated  
465 here with different applications cases.

466 For the direct determination of heavy elements ( $Z > 70$ ) in hydrocarbon matrices, the ICP-MS/MS  
467 was less sensitive than the ICP-HRMS when the direct introduction of organic substances was  
468 used. For light elements ( $Z < 40$ ), the sensitivity was similar or better using ICP-MS/MS and for  
469 interfered elements (Si, S, Ca, Fe), the use of the two quadrupoles combined to the octopole  
470 reaction/collision cell (ORC) with He, O<sub>2</sub> or H<sub>2</sub> gave similar or better detection limits (LOD) than  
471 the ICP-HRMS in medium resolution. The results obtained with the ICP-MS/MS gave good  
472 performance with detection limit within the range of 0.004 µg/kg (V) to 0.9 µg/kg (Al) and  
473 appeared in the lowest values published in the literature using ICP-MS/MS in organic solvents.

474 Sulfur at very low levels in reformates was successfully monitored in the oxygen mode using the  
475 oxide ion ( $^{32}\text{S} \rightarrow ^{48}\text{SO}$ ). The background equivalent concentration (BEC) origin was attributed to  
476 solvent contamination by sulfur and was confirmed by UVF method. Using He, O<sub>2</sub> or H<sub>2</sub> as  
477 reactant gas, the ICP-MS/MS method easily confirmed Ni and V concentrations measured using  
478 wavelength dispersive X-rays fluorescence (WDXRF) and allowed the determination of 14  
479 elements in the asphaltene fraction, with concentrations ranging from 0.3 mg/kg (Al and Pb) to  
480 37.4 mg/kg for Fe.

481 For speciation of Ni, V and S, GPC-ICP-MS/MS is particularly powerful using O<sub>2</sub> both for high  
482 (vacuum residue) and low (HDT vacuum residue) contaminated heavy products. Contrary to  
483 GPC-ICP-HRMS where two injections of sample were required (medium resolution for S and V  
484 and low resolution for Ni), GPC-ICP-MS/MS easily allowed the acquisition of the 3 elements in  
485 one mode during the same run and considerably enhancing the sample throughput. This paper  
486 clearly demonstrates new opportunities of the ICP-MS/MS in the oil industry using direct

487 injection of petroleum feedstock's and products after dilution in hydrocarbon solvent for total  
488 determination of metals but also for advanced speciation in non-distillable fractions.  
489

490           **5 Acknowledgments**

491   The help of Leslie Joguet-Valentin and Floriane Lovery (IFPEN, Solaize, France) was very  
492   useful for the S value of the PremiSolv by UVF and the WDXRF value of Ni and V for the  
493   asphaltene fraction respectively.

494

495           **6 References**

- 496 [1] Korn, Maria das Graças Andrade, Santos, Denilson Santana Sodr  dos, B. Welz, Vale, Maria  
497 Goretı Rodrigues, A.P. Teixeira, Lima, Daniel de Castro, Ferreira, S rgio Luis Costa,  
498 Atomic spectrometric methods for the determination of metals and metalloids in automotive  
499 fuels--a review, *Talanta* 73 (1) (2007) 1–11. <https://doi.org/10.1016/j.talanta.2007.03.036>.
- 500 [2] C.P. Lienemann, Analysis of trace metals in petroleum products, state of the art, *Oil & Gas  
501 Science and Technology-Revue de l Institut Francais du Petrole* 60 (6) (2005) 951–965.
- 502 [3] R. S nchez, J.L. Todol , C.-P. Lienemann, J.-M. Mermet, Determination of trace elements in  
503 petroleum products by inductively coupled plasma techniques: A critical review,  
504 *Spectrochimica Acta Part B: Atomic Spectroscopy* 88 (2013) 104–126.  
505 <https://doi.org/10.1016/j.sab.2013.06.005>.
- 506 [4] A. Leclercq, A. Nonell, Todol  Torr , Jos  Luis, C. Bresson, L. Vio, T. Vercoouter, F.  
507 Chartier, Introduction of organic/hydro-organic matrices in inductively coupled plasma  
508 optical emission spectrometry and mass spectrometry: a tutorial review. Part II. Practical  
509 considerations, *Analytica Chimica Acta* 885 (2015) 57–91.  
510 <https://doi.org/10.1016/j.aca.2015.04.039>.
- 511 [5] P. Dufresne, Hydroprocessing catalysts regeneration and recycling, *Applied Catalysis A-  
512 General* 322 (2007) 67–75. <https://doi.org/10.1080/01614949608006454>.
- 513 [6] Palmer S. E., Baker E.W., *Science* (1978) 49–51.
- 514 [7] A. Treibs, On the Chromophores of porphyrin systems, *Annals of the New York Academy  
515 of Sciences* 206 (1973) 97–115. <https://doi.org/10.1111/j.1749-6632.1973.tb43207.x>.
- 516 [8] G. Caumette, C.P. Lienemann, I. Merdrignac, B. Bouyssi re, R. Lobinski, Element  
517 speciation analysis of petroleum and related materials, *J Anal Atom Spectrom* 24 (3) (2009)  
518 263–276. <https://doi.org/10.1039/b817888g>.
- 519 [9] F. Chainet, L. Le Meur, C.-P. Lienemann, J. Ponthus, M. Courtiade, Donard, Olivier  
520 Fran ois Xavier, Characterization of silicon species issued from PDMS degradation under  
521 thermal cracking of hydrocarbons: Part 2 – Liquid samples analysis by a multi-technical  
522 approach based on gas chromatography and mass spectrometry, *Fuel* 116 (2014) 478–489.  
523 <https://doi.org/10.1016/j.fuel.2013.08.010>.

- 524 [10] B. Didillon, J. Cosyns, C. Cameron, D. Uzio, P. Sarrazin, J.P. Boitiaux, Industrial evaluation  
525 of selective hydrogenation catalyst poisoning, *Catalyst Deactivation* 1997 111 (1997) 447–  
526 454. <https://doi.org/10.2516/ogst:2007006>.
- 527 [11] A. Doyle, A. Saavedra, M.L.B. Tristão, R.Q. Aucelio, Determination of S, Ca, Fe, Ni and V  
528 in crude oil by energy dispersive X-ray fluorescence spectrometry using direct sampling on  
529 paper substrate, *Fuel* 162 (2015) 39–46. <https://doi.org/10.1016/j.fuel.2015.08.072>.
- 530 [12] A. Cinosi, N. Andriollo, G. Pepponi, D. Monticelli, A novel total reflection X-ray  
531 fluorescence procedure for the direct determination of trace elements in petrochemical  
532 products, *Anal Bioanal Chem* 399 (2) (2011) 927–933. <https://doi.org/10.1007/s00216-010-4352-x>.
- 534 [13] J. Nelson, G. Gilleland, L. Poirier, D. Leong, P. Hajdu, F. Lopez-Linares, Elemental  
535 Analysis of Crude Oils Using Microwave Plasma Atomic Emission Spectroscopy, *Energy &*  
536 *Fuels* 29 (9) (2015) 5587–5594. <https://doi.org/10.1021/acs.energyfuels.5b01026>.
- 537 [14] A. Harhira, J. El Haddad, A. Blouin, M. Sabsabi, Rapid Determination of Bitumen Content  
538 in Athabasca Oil Sands by Laser-Induced Breakdown Spectroscopy, *Energy Fuels* 32 (3)  
539 (2018) 3189–3193. <https://doi.org/10.1021/acs.energyfuels.7b03821>.
- 540 [15] L. Poirier, J. Nelson, D. Leong, L. Berhane, P. Hajdu, F. Lopez-Linares, Application of ICP-  
541 MS and ICP-OES on the Determination of Nickel, Vanadium, Iron, and Calcium in  
542 Petroleum Crude Oils via Direct Dilution, *Energy Fuels* 30 (5) (2015) 3783–3790.  
543 <https://doi.org/10.1021/acs.energyfuels.5b02997>.
- 544 [16] S. Dreyfus, C. Pecheyran, C. Magnier, A. Prinzhofer, C.P. Lienemann, O.F.X. Donard,  
545 Direct trace and ultra-trace metals determination in crude oil and fractions by inductively  
546 coupled plasma mass spectrometry, *Elemental Analysis of Fuels and Lubricants: Recent*  
547 *Advances and Future Prospects* 1468 (2005) 51–58.
- 548 [17] G. Caumette, C.-P. Lienemann, I. Merdrignac, B. Bouyssièrre, R. Lobinski, Fractionation and  
549 speciation of nickel and vanadium in crude oils by size exclusion chromatography-ICP MS  
550 and normal phase HPLC-ICP MS, *J Anal Atom Spectrom* 25 (7) (2010) 1123.  
551 <https://doi.org/10.1039/c003455j>.
- 552 [18] F. Chainet, C.-P. Lienemann, J. Ponthus, C. Pécheyran, J. Castro, E. Tessier, Donard, Olivier  
553 François Xavier, Towards silicon speciation in light petroleum products using gas  
554 chromatography coupled to inductively coupled plasma mass spectrometry equipped with a

- 555 dynamic reaction cell, *Spectrochimica Acta Part B: Atomic Spectroscopy* 97 (2014) 49–56.  
556 <https://doi.org/10.1016/j.sab.2014.04.010>.
- 557 [19] R. Sánchez, J.L. Todolí, C.-P. Lienemann, J.-M. Mermet, Universal calibration for metal  
558 determination in fuels and biofuels by inductively coupled plasma atomic emission  
559 spectrometry based on segmented flow injection and a 350 °C heated chamber, *J Anal Atom*  
560 *Spectrom* 27 (6) (2012) 937. <https://doi.org/10.1039/c2ja10336b>.
- 561 [20] A. Leclercq, A. Nonell, Todolí Torró, José Luis, C. Bresson, L. Vio, T. Vercoouter, F.  
562 Chartier, Introduction of organic/hydro-organic matrices in inductively coupled plasma  
563 optical emission spectrometry and mass spectrometry: A tutorial review. Part I. Theoretical  
564 considerations, *Analytica Chimica Acta* 885 (2015) 33–56.  
565 <https://doi.org/10.1016/j.aca.2015.03.049>.
- 566 [21] P. Pohl, N. Vorapalawut, B. Bouyssiére, H. Carrier, R. Lobinski, Direct multi-element  
567 analysis of crude oils and gas condensates by double-focusing sector field inductively  
568 coupled plasma mass spectrometry (ICP MS), *J Anal Atom Spectrom* 25 (5) (2010) 704.  
569 <https://doi.org/10.1039/c000658k>.
- 570 [22] J. Heilmann, S.F. Boulyga, K.G. Heumann, Development of an isotope dilution laser  
571 ablation ICP-MS method for multi-element determination in crude and fuel oil samples, *J.*  
572 *Anal. At. Spectrom.* 24 (4) (2009) 385–390. <https://doi.org/10.1039/B819879A>.
- 573 [23] A. Desprez, B. Bouyssiére, C. Arnaudguilhem, G. Krier, L. Vernex-Loiset, P. Giusti, Study  
574 of the Size Distribution of Sulfur, Vanadium, and Nickel Compounds in Four Crude Oils and  
575 Their Distillation Cuts by Gel Permeation Chromatography Inductively Coupled Plasma  
576 High-Resolution Mass Spectrometry, *Energy & Fuels* 28 (6) (2014) 3730–3737.  
577 <https://doi.org/10.1021/ef500571f>.
- 578 [24] S. Gutierrez Sama, A. Desprez, G. Krier, C.-P. Lienemann, J. Barbier, R. Lobinski, C.  
579 Barrere-Mangote, P. Giusti, B. Bouyssiére, Study of the Aggregation of Metal Complexes  
580 with Asphaltenes Using Gel Permeation Chromatography Inductively Coupled Plasma High-  
581 Resolution Mass Spectrometry, *Energy Fuels* 30 (9) (2016) 6907–6912.  
582 <https://doi.org/10.1021/acs.energyfuels.6b00559>.
- 583 [25] L. Balcaen, E. Bolea-Fernandez, M. Resano, F. Vanhaecke, Inductively coupled plasma -  
584 Tandem mass spectrometry (ICP-MS/MS): A powerful and universal tool for the



- 585 interference-free determination of (ultra)trace elements – A tutorial review, *Analytica*  
586 *Chimica Acta* 894 (2015) 7–19. <https://doi.org/10.1016/j.aca.2015.08.053>.
- 587 [26] L. Balcaen, G. Woods, M. Resano, F. Vanhaecke, Accurate determination of S in organic  
588 matrices using isotope dilution ICP-MS/MS, *J. Anal. At. Spectrom.* 28 (1) (2013) 33–39.  
589 <https://doi.org/10.1039/c2ja30265a>.
- 590 [27] R.S. Amais, Amaral, Clarice D. B., L.L. Fialho, D. Schiavo, J.A. Nóbrega, Determination of  
591 P, S and Si in biodiesel, diesel and lubricating oil using ICP-MS/MS, *Anal. Methods* 6 (13)  
592 (2014) 4516. <https://doi.org/10.1039/c4ay00279b>.
- 593 [28] E. Bolea-Fernandez, L. Balcaen, M. Resano, F. Vanhaecke, Overcoming spectral overlap via  
594 inductively coupled plasma-tandem mass spectrometry (ICP-MS/MS). A tutorial review, *J.*  
595 *Anal. At. Spectrom.* 32 (9) (2017) 1660–1679. <https://doi.org/10.1039/C7JA00010C>.
- 596 [29] Tomoko Vincent, Determination of ultratrace elements in photoresist solvents using the  
597 Thermo Scientific iCAP TQs ICP-MS (Application note 43374), 2018 (accessed 15  
598 November 2018).
- 599 [30] Y. Kitamanki, Y. Zhu, M. Numata, Accurate Characterization of Sulfur in Biodiesel Fuel  
600 Certified Reference Material, *J. Jpn. Petrol. Inst.* 59 (6) (2016) 317–321.  
601 <https://doi.org/10.1627/jpi.59.317>.
- 602 [31] C. Walkner, R. Gratzner, T. Meisel, S.N.H. Bokhari, Multi-element analysis of crude oils  
603 using ICP-QQQ-MS, *Organic Geochemistry* 103 (2017) 22–30.  
604 <https://doi.org/10.1016/j.orggeochem.2016.10.009>.
- 605 [32] W. Yang, J.F. Casey, Y. Gao, A new sample preparation method for crude or fuel oils by  
606 mineralization utilizing single reaction chamber microwave for broader multi-element  
607 analysis by ICP techniques, *Fuel* 206 (2017) 64–79.  
608 <https://doi.org/10.1016/j.fuel.2017.05.084>.
- 609 [33] A. Vetere, D. Pröfrock, W. Schrader, Quantitative and Qualitative Analysis of Three Classes  
610 of Sulfur Compounds in Crude Oil, *Angew. Chem. Int. Ed Engl.* 56 (36) (2017) 10933–  
611 10937. <https://doi.org/10.1002/anie.201703205>.
- 612 [34] F. Chainet, L. Le Meur, C.-P. Lienemann, M. Courtiade, J. Ponthus, L. Brunet-Errard,  
613 Donard, Olivier François Xavier, Degradation processes of polydimethylsiloxane under  
614 thermal cracking conditions of hydrocarbons in an experimental pilot plant followed by size  
615 exclusion chromatography coupled to inductively coupled plasma high resolution mass

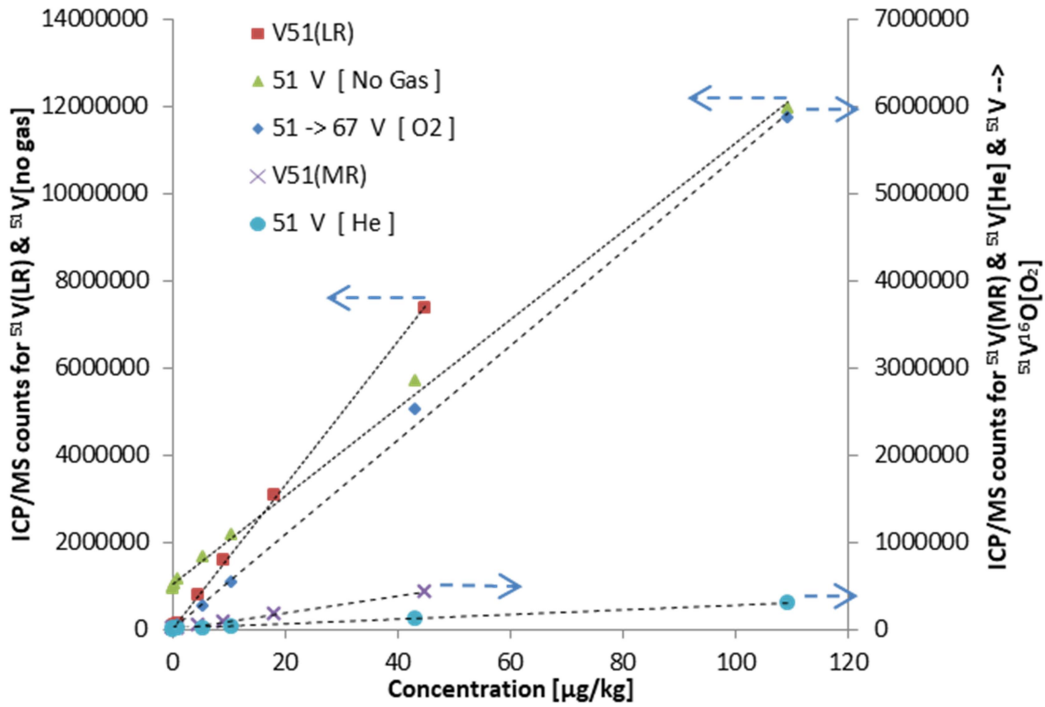
- 616 spectrometry, *Fuel Processing Technology* 104 (2012) 300–309.  
617 <https://doi.org/10.1016/j.fuproc.2012.05.029>.
- 618 [35] J. Barbier, J. Marques, G. Caumette, I. Merdrignac, B. Bouyssiere, R. Lobinski, C.-P.  
619 Lienemann, Monitoring the behaviour and fate of nickel and vanadium complexes during  
620 vacuum residue hydrotreatment and fraction separation, *Fuel Processing Technology* 119  
621 (2014) 185–189. <https://doi.org/10.1016/j.fuproc.2013.11.004>.
- 622 [36] P. Giusti, Y.N. Ordonez, C.P. Lienemann, D. Schaumloffel, B. Bouyssiere, R. Lobinski,  $\mu$ -  
623 Flow-injection-ICP collision cell MS determination of molybdenum, nickel and vanadium in  
624 petroleum samples using a modified total consumption micronebulizer, *J Anal Atom*  
625 *Spectrom* 22 (1) (2007) 88–92.
- 626 [37] V. Thomsen, D. Schatzlein, D. Mercurio, Limits of detection in spectroscopy, *Spectroscopy*  
627 18 (12) (2003) 112–114.
- 628 [38] R.H. Filby, S.D. Olsen, A comparison of instrumental neutron activation analysis and  
629 inductively coupled plasma-mass spectrometry for trace element determination in petroleum  
630 geochemistry, *Journal of Radioanalytical and Nuclear Chemistry* 180 (1994) 285–294.
- 631 [39] C. Duyck, N. Miekeley, Porto da Silveira, Carmem L., P. Szatmari, Trace element  
632 determination in crude oil and its fractions by inductively coupled plasma mass spectrometry  
633 using ultrasonic nebulization of toluene solutions, *Spectrochimica Acta Part B: Atomic*  
634 *Spectroscopy* 57 (12) (2002) 1979–1990. [https://doi.org/10.1016/S0584-8547\(02\)00171-4](https://doi.org/10.1016/S0584-8547(02)00171-4).  
635

## 7 Tables and Figures

636		
637		
638	Table 1: Characteristics of the petroleum cuts provided for the various experiments. ....	8
639	Table 2: Operating conditions for total analysis using ICP-MS apparatus .....	10
640	Table 3: BEC [ $\mu\text{g}/\text{kg}$ ] of $^{32\rightarrow 48}\text{S}$ obtained for each solvent and plasma conditions. ....	19
641	Table 4: Concentration obtained by WDXRF and ICP-MS/MS for the asphaltene fraction .....	21
642		
643	Figure 1: Comparison of detection limits obtained using diameters 1.0 and 1.5 mm for two	
644	injectors proposed for the ICP-MS/MS.....	13
645	Figure 2: Calibration curves for S using ICP-HRMS or ICP-MS/MS (Arrows indicate the correct	
646	axis for all calibration curves).....	14
647	Figure 3: Calibration curves for Si using ICP-HRMS or ICP-MS/MS (Arrows indicate the correct	
648	axis for all calibration curves).....	15
649	Figure 4: Calibration curves for Fe using ICP-HRMS or ICP-MS/MS .....	15
650	Figure 5: Comparison of Background Equivalent Concentration (a) and Limit of Detection (b) for	
651	various elements between ICP-HRMS and ICP-MS/MS detection. ....	17
652	Figure 6: Comparison of GPC-ICP-MS/MS and GPC-ICP-HRMS chromatograms for Ni,	
653	injecting a VR with Ni content around 60 mg/kg .....	22
654	Figure 7: Comparison of GPC-ICP-MS/MS and GPC-ICP-HRMS chromatograms for S (a) and V	
655	(b).....	24
656	Figure 8: Comparison of GPC-ICP-MS/MS and GPC-ICP--HRMS chromatograms for Ni,	
657	injecting the HDT VR with Ni content around 3 mg/kg.....	25
658		
659	Figure S 1: Calibration curves for Ni ( $^{58\rightarrow 58}\text{Ni}$ and $^{60\rightarrow 60}\text{Ni}$ ) and V using ICP-HRMS or ICP-	
660	MS/MS (Arrows indicate the correct axis for all calibration curves) .....	36
661		
662		

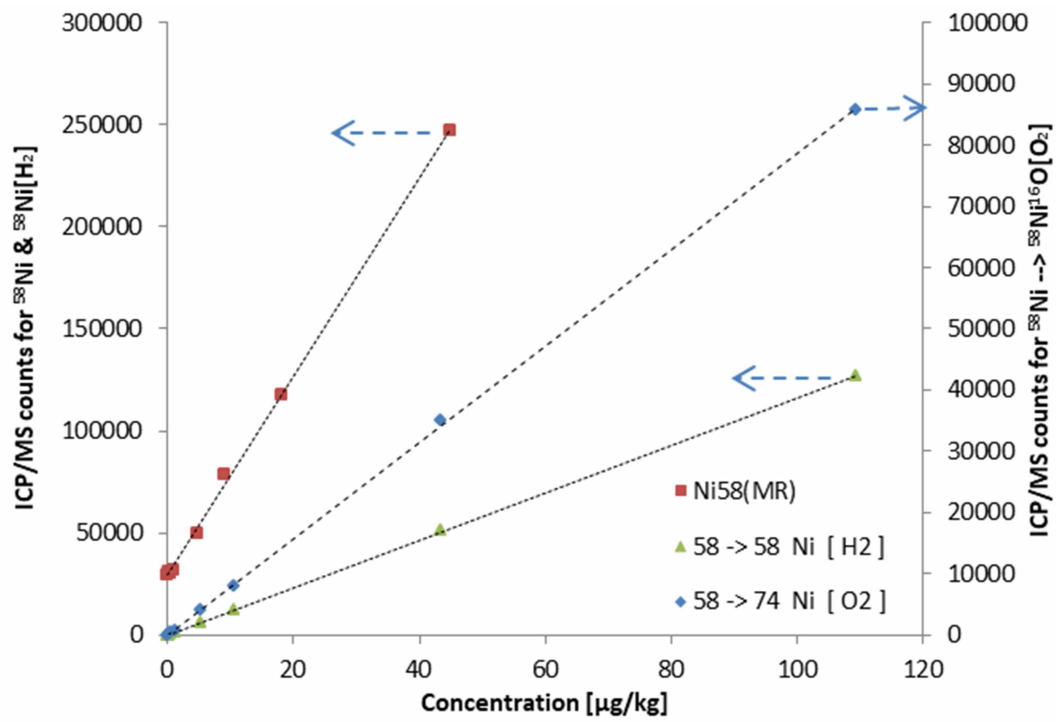
663 **8 Supplementary material**

664

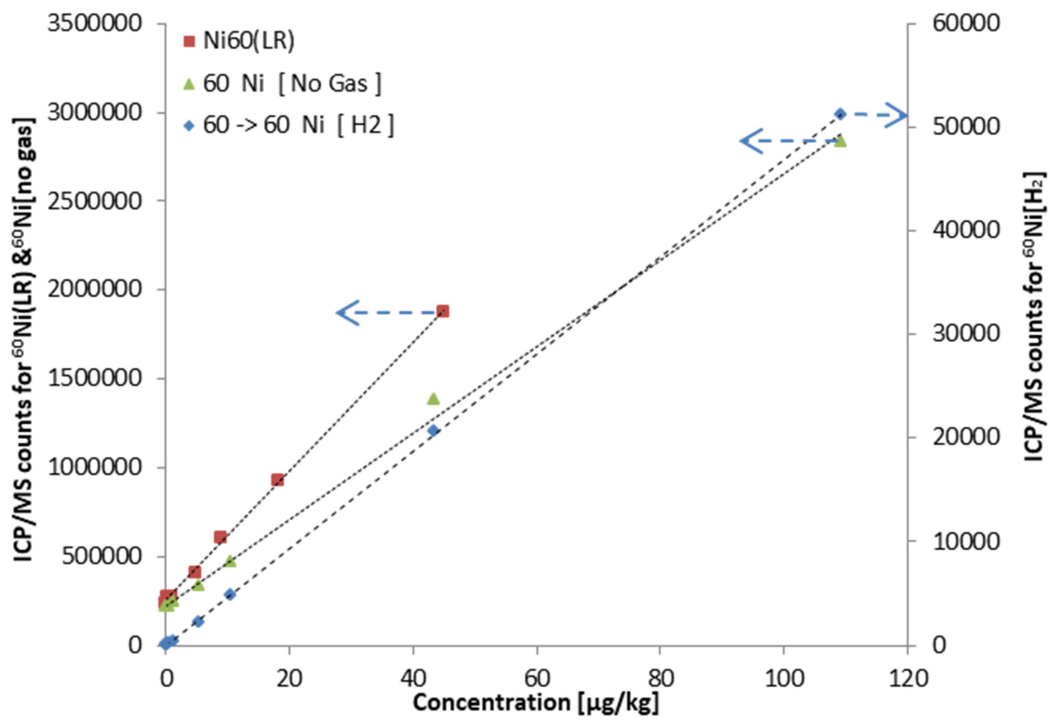


665

666



667



668

669 Figure S 1: Calibration curves for Ni ( $^{58}\text{Ni}$  and  $^{60}\text{Ni}$ ) and V using ICP-HRMS or ICP-MS/MS  
 670 (Arrows indicate the correct axis for all calibration curves)